Amyloid-β(1−42) Rapidly Forms Protofibrils and Oligomers by Distinct Pathways in Low Concentrations of Sodium Dodecylsulfate†

Vijayaraghavan Rangachari, Brenda D. Moore, Dana Kim Reed, Leilani K. Sonoda, Alexander W. Bridges, Erin Conboy, David Hartigan, and Terrone L. Rosenberry*

Department of Neuroscience, Mayo Clinic College of Medicine, 4500 San Pablo Road, Jacksonville, Florida 32224

Received June 19, 2007; Revised Manuscript Received August 10, 2007

ABSTRACT: Alzheimer's disease (AD) is characterized by large numbers of senile plaques in the brain that consist of fibrillar aggregates of 40- and 42-residue amyloid-β (Aβ) peptides. However, the degree of dementia in AD correlates better with the concentration of soluble Aβ species assayed biochemically than with histologically determined plaque counts, and several investigators now propose that soluble aggregates of Aβ are the neurotoxic agents that cause memory deficits and neuronal loss. These endogenous aggregates are minor components in brain extracts from AD patients and transgenic mice that express human Aβ, but several species have been detected by gel electrophoresis in sodium dodecylsulfate (SDS) and isolated by size exclusion chromatography (SEC). Endogenous Aβ aggregation is stimulated at cellular interfaces rich in lipid rafts, and anionic micelles that promote Aβ aggregation *in vitro* may be good models of these interfaces. We previously found that micelles formed in dilute SDS (2 mM) promote Aβ(1−40) fiber formation by supporting peptide interaction on the surface of a single micelle complex. In contrast, here we report that monomeric Aβ(1−42) undergoes an immediate conversion to a predominant β-structured conformation in 2 mM SDS which does not proceed to amyloid fibrils. The conformational change is instead rapidly followed by the near quantitative conversion of the 4 kDa monomer SDS gel band to 8−14 kDa bands consistent with dimers through tetramers. Removal of SDS by dialysis gave a shift in the predominant SDS gel bands to 30−60 kDa. While these oligomers resemble the endogenous aggregates, they are less stable. In particular, they do not elute as discrete species on SEC, and they are completed disaggregated by boiling in 1% SDS. It appears that endogenous oligomeric Aβ aggregates are stabilized by undefined processes that have not yet been incorporated into *in vitro* Aβ aggregation procedures.

The brains of patients with Alzheimer's disease (AD)[1] contain large numbers of fibrillar amyloid deposits in the form of senile plaques (*1*). The fibrils in senile plaques are composed of peptides called Aβ(1−40) and Aβ(1−42) (*2*, *3*) that are produced by proteolysis of cellular amyloid precursor protein (APP) (*4*). The peptides are identical except for an additional dipeptide segment Ile-Ala at the C-terminus of Aβ(1−42) that extends beyond the 40-residue sequence in Aβ(1−40). As originally suggested by the amyloid cascade hypothesis (*5*), it appears likely that Aβ peptide aggregates initiate cellular events that lead to neurodegeneration and AD. The strongest evidence supporting this hypothesis comes from the identification of numerous mutations linked to early onset familial AD (FAD) (*6*). All reported FAD mutations increase either the overall production of Aβ, the level of the more amyloidogenic Aβ(1−42) relative to Aβ(1−40) (reviewed in (*6*)), or the propensity of a mutated Aβ to form amyloid aggregates (*7*).

The degree of dementia in AD correlates much better with the concentration of soluble Aβ species assayed biochemically than with histologically determined plaque counts (see ref *8*). As a consequence, a number of investigators now propose that soluble aggregates of Aβ, rather than insoluble amyloid fibrils, may be responsible for synaptic dysfunction and learning deficits in the brains of AD patients and AD animal models (*8*−*14*). These endogenous soluble Aβ aggregates are present at low levels, making their identification and characterization difficult, but several species in extracts of AD brains have been detected as bands on immunoblots of SDS-PAGE gels (*15*). Similar bands also were observed in samples of Aβ immunoprecipitated from the conditioned medium of CHO cells transfected with APP cDNA (*13*, *16*, *17*) and in brain extracts from transgenic Tg2576 mice that express a mutant human APP and substantial levels of Aβ (*12*, *14*, *18*). The apparent molecular masses of the bands corresponded to multiples of 4 kDa Aβ monomers and ranged from dimers to dodecamers, and the

† This work was supported by Robert and Clarice Smith Fellowship awards to V.R and B.D.P, by an award from the American Heart Association, National Center (0535185N) to V.R., and by Mayo Clinic Summer Undergraduate Research Fellowships to A.W.B., E.C., and D.H.

* To whom the correspondence to be addressed. Tel: 904 953 7375. Fax: 904 953 7370. E-mail: Rosenberry@mayo.edu.

[1] Abbreviations: AD, Alzheimer's disease; AFM, atomic force microscopy; APP, amyloid precursor protein; CD, circular dichroism; CHO, Chinese hamster ovary; CMC, critical micelle concentration; DOPG, 1,2-dioleoyl-*sn*-glycero-3-(phospho-*rac*-1-glycerol); EM, electron microscopy; FAD, early-onset familial AD; HFIP, hexafluoro-2-propanol; 2−4mers, dimer, trimer, and tetramer forms of Aβ(1-42); LDS, lithium dodecylsulfate; NM domain; N-terminal and middle domain; PAGE, polyacrylamide gel electrophoresis; PBS, 150 mM NaCl, 25 mM sodium phosphate (pH 7.0); PICUP, photo-induced cross-linking of unmodified proteins; SD, standard deviation; SDS, sodium dodecylsulfate; SEC, size exclusion chromatography.

10.1021/bi701213s CCC: $37.00
Published on Web 10/02/2007

species collectively have thus been designated as Aβ oligomers. While some of these oligomers could have been derived from larger aggregates that were dissociated by SDS during SDS-PAGE analysis, fractionation by size exclusion chromatography (SEC) in the absence of detergent showed that this was not the case. They were isolated as discrete species at elution volumes consistent with their apparent masses on SDS-PAGE (*13*, *14*, *19*). The isolated oligmers are of great interest, as they appear to potently inhibit hippocampal long-term potentiation (*13*, *17*) and disrupt cognitive function (*14*, *20*).

The isolation of Aβ oligomers following aggregation of the synthetic peptides *in vitro* has been more elusive. SDS-PAGE bands in the dimer to tetramer range are readily observed with Aβ(1−42) (*21*−*25*), but most of the Aβ recovered following SEC of the aggregation reactions appeared to correspond to large aggregates in the void volume or to monomers (*24*). Aβ(1−42) oligomers that gave broad SDS-PAGE bands roughly in the range of octamers to dodecamers were recently obtained by including dilute SDS in the aggregation reaction (*26*). The size of these oligomers remained stable after removal of the SDS by dialysis, and SEC of the dialyzed sample gave an elution peak. However, the authors did not report whether discrete SDS-PAGE bands were separated by this fractionation. Although SDS is often viewed as a denaturant that destroys native protein conformation, it provides an anionic micellar interface that was shown to accelerate the aggregation of both Aβ(1−40) and Aβ(1−42) over a limited range of low SDS concentrations at or below the critical micelle concentration (CMC) (*27*). We recently reported that dilute SDS (2 mM) accelerates the formation of soluble fibers by Aβ-(1−40) (*28*). In contrast, SDS concentrations well above the CMC stabilized the peptide in an α-helical structure that did not aggregate. Here we examine the effects of dilute SDS on the aggregation of Aβ(1−42). Fiber formation was promoted at an SDS concentration (0.5 mM) even lower than that observed with Aβ(1−40). However, a slightly higher concentration of SDS (2 mM) induced very rapid conversion of Aβ(1−42), but not Aβ(1−40), to a conformation rich in β-structure that formed oligomers but not fibers.

EXPERIMENTAL PROCEDURES

Materials. Aβ(1−40) and Aβ(1−42) were synthesized on preloaded NovaSyn TGA resins (EMD Novabiochem, San Diego, CA) utilizing orthogonal Fmoc solid-phase chemistry by the Peptide Synthesis Facility at the Mayo Clinic (Rochester, MN). Two steps were taken to improve yields of Aβ(1−42). First, the solid-phase synthesis utilized a pseudoproline (oxazolidine) dipeptide Fmoc-Gly-Ser($\psi^{Me,Me}$ Pro)-OH (*29*) that was converted to wild type sequence Gly-25 and Ser-26 after trifluoroacetic acid cleavage of the peptide from the TGA resin. Second, HPLC purification of the peptide was omitted in lieu of purification by size exclusion chromatography (SEC) as described below. MALDI-TOF mass spectrometry revealed >90% purity of both peptides. SDS, bovine serum albumin, and thioflavin T were procured from Sigma-Aldrich (St. Louis, MO). All other buffers and salts were obtained from Fisher Inc.

Preparation of Aβ Monomers. Lyophilized stocks of Aβ peptides were stored at −80 °C desiccated. Samples of Aβ-(1−40) were reconstituted in 0.1 M Tris-HCl (pH 8.0) and purified by size exclusion chromatography (SEC) on Superdex 75 as described previously (*28*). Aβ(1−42) was dissolved at 0.5−2.0 mM either in 1:1 hexafluoro-2-propanol (HFIP)/water or in 30 mM NaOH (*30*) 15 min prior to SEC on Superdex 75. Yields of monomeric Aβ(1−42) in SEC fractions were higher following dissolution in NaOH, and peptide integrity was again confirmed by MALDI-TOF mass spectrometry. Monomeric Aβ(1−42) was stored at 4 °C and used within 1 day of SEC purification in all the experiments. Concentrations of Aβ were determined by UV absorbance with a calculated extinction coefficient of 1450 cm^{-1} M^{-1} at 276 nm (*31*). Relative peptide concentrations were determined by BCA assay (Pierce, Rockford, IL).

Size Exclusion Chromatography (SEC). Column preparation and use generally were described previously (*31*). In brief, samples (0.5−1.0 mL) were loaded on to a 1 × 30 cm Superdex 75 HR 10/30 column (Amersham Pharmacia) attached to either an AKTA FPLC or a Pharmacia LKB system. The column was pre-equilibrated in 20 mM Tris-HCl (pH 8.0) at 25 °C and run at a flow rate of 0.5 mL/min. One minute fractions were collected. Cytochrome *c* (Sigma-Aldrich) (12.5 kDa) was used for M_W calibration. Its elution volume relative to Aβ(1−42) was identical with or without addition of 150 mM NaCl, but its recovery was much higher with NaCl.

Aβ Aggregation Reactions. All reactions and measurements were made at room temperature (25 °C) unless otherwise noted. SDS stock solutions were filtered (0.2 μm cellulose acetate filters, VWR Scientific Products, West Chester, PA). Reactions were initiated in siliconized Eppendorf tubes by incubating appropriate concentrations of freshly purified Aβ monomer in buffer in the presence or absence of SDS without agitation. Aggregation kinetic parameters were obtained by monitoring the reaction with thioflavin T and fitting fluorescence (F) data points to the sigmoidal curve in eq 1 (*32*) using Origin 5.0. In this equation, t is time, $t_{0.5}$ is the time to reach half-maximal thioflavin T fluorescence, and a, b, and $t_{0.5}$ are constant parameters whose values are obtained from the fitting process. Data points were unweighted. Lag times were defined as described in (*32*) and were equal to $t_{0.5} - 2b$ for each fitted curve.

$$F = \frac{a}{1 + e^{-[(t - t_{0.5})/b]}} \quad (1)$$

Polyacrylamide Gel Electrophoreses (PAGE) and Immunoblotting. Unless otherwise noted, samples were adjusted to loading buffer (NuPAGE, Invitrogen Inc, Carlsbad, CA) containing 1% LDS, applied without heating to NuPAGE pre-cast 4−12% acrylamide gels containing bis-Tris, and resolved in NuPAGE MES SDS running buffer with 0.1% SDS. Dye-linked M_W markers (SeeBlue Plus2 Prestained Standards, Invitrogen) were run in parallel for calibration. Gels were electroblotted onto 0.45 μm Immobilon PVDF membranes (Millipore, Bedford, MA). Blots were blocked overnight with PBS containing 5% nonfat dry milk and probed (1.5−3 h) with 1:1000−1:2500 dilutions of monoclonal antibodies 6E10 (Senetek, Maryland Heights, MO) or Ab9 (*33*), both of which detect Aβ(1−16). Blots were then incubated with an anti-mouse horseradish peroxide (HRP) conjugate and developed with ECL reagent (GE

Healthcare, Buckinghamshire, UK). Where noted, blots were boiled in a microwave oven in PBS for 10 min before blocking in PBS with milk.

ELISA Measurement of Aβ. To quantify Aβ(1−42) bands in SDS-PAGE gels, slices from each lane spanning the range of monomer (0−6 kDa), 2−4mers (6−14 kDa), and larger aggregates (14 kDa − loading well) were excised and incubated with 0.2% diethylamine overnight to largely dissociate Aβ aggregates and extract Aβ from the gel slices. Samples were neutralized with 0.5 M Tris-HCl, and Aβ(1−42) was measured by a sandwich ELISA system (*34*) that utilized Ab9 as the capture antibody and monoclonal antibody 4G8 (Senetek, Maryland Heights, MO), which recognizes the epitope Aβ_{18-22}, for detection. The 4G8 detection antibody was conjugated to HRP with the EZ-Link Plus Activated Peroxidase Kit (Pierce, Rockford, IL) according to the manufacturer's instructions. Triplicate assays were conducted by applying aliquots to microtiter plates precoated with capture antibody and incubating at 4 °C overnight. Plates were then washed, incubated with the detection antibody for 3 h at room temperature, and developed with tetramethylbenzidine.

Circular Dichroism (CD) Spectroscopy. CD spectra were obtained in the far UV region with a Jasco J-810 spectropolarimeter (Jasco Inc., Easton, MD) in continuous scan mode (260−190 nm) and a 0.1 cm path-length quartz cuvette (Hellma). The acquisition parameters were 50 nm/min with 8 s response times, 1 nm bandwidth, and 0.1 nm data pitch, and data sets were averaged over three scans unless otherwise noted. Spectra of appropriate solvent blanks were subtracted from the data sets. The corrected, averaged spectra were smoothed using the 'means-movement' algorithm with a convolution width of 25 in the Jasco spectra analysis program. Data were normalized to mean residue ellipticity using the equation, $[\theta] = [\theta]_{obs} \times (MRW/10lc)$, where MRW is the mean residue molecular weight of Aβ(1−42) (4513 g/mol divided by 42 residues), l is the optical path length (cm), and c is the concentration (g/cm^3).

Fluorescence Spectroscopy. Thioflavin T fluorescence measurements were performed as described previously (*31*, *35*). Briefly, the fluorescence (F) was monitored in a microcuvette with a Perkin-Elmer LS-50B luminescence spectrometer after 15-fold of Aβ(1−40) samples into 5 mM Tris-HCl (pH 8.0) containing 5 μM thioflavin T. Continuous measurements of F were taken for 10−15 min with the excitation wavelength fixed at 450 nm and the emission fixed at 480 nm, and the excitation and emission slits set at 10 nm, and the average F value was determined. The fluorescence of solvent blanks was subtracted.

Electron Microscopy (EM). Samples of Aβ aggregates were applied to 200 mesh Formvar-coated copper grids (Ernest F. Fullam, Inc, Latham, NY) and incubated for 10−15 min at room temperature. The sample was then wicked off with lens paper, washed briefly by placing the grid face down on a droplet of water, and stained by transferring the grid face down to a droplet of 2% uranyl acetate (Polysciences, Inc., Warrington, PA) for 5−10 min before wicking off the solution and air drying. Grids were visualized in a Philips EM208S transmission electron microscope.

Atomic Force Microscopy (AFM). Images were obtained as described previously (*36*). Briefly, the samples were incubated for 15 min on freshly cleaved mica that had been modified with 3′-(aminopropyl)triethoxysilane (APTES), and the disk was briefly washed with water and then dried over desiccant before imaging. A NanoScope III controller with a Mulitmode AFM (Veeco Instruments Inc, Chadds Ford, PA) was used for imaging by ambient tapping mode. Images were obtained in either amplitude mode or height mode, where increasing brightness indicates greater damping of cantilever oscillation (*37*) or increasing feature height, respectively. Height images were "flattened," and particle heights were collected using the "section" function of the NanoScope (version 613b21) software. Particle height averages were based on at least five preparations; heights of $<$1.0 nm or $>$5.0 nm were rejected.

RESULTS

SDS-Stable Oligomers Are Formed More Readily by Aβ(1−42) Than by Aβ(1−40) and Are Generated during Incubation in the Absence of SDS. To avoid contamination with preexisting aggregates, Aβ monomers were isolated by SEC prior to all experiments. Although there has been some controversy about whether the isolated Aβ is truly monomeric, translational diffusion measurements by NMR (*38*) and M_w measurements by multiangle light scattering (*39*, *40*) have confirmed the monomeric assignment.

Several recent reports have emphasized the presence of SDS-stable oligomers in tissue and cell extracts, but the relationship of these oligomers to aggregates generated *in vitro* from Aβ monomers has remained unclear. SDS-PAGE bands in the Aβ dimer/trimer and particularly tetramer region were observed in early analyses of several synthetic Aβ peptides, including Aβ(1−42) (*21*) and Aβ(x-43) (*41*), and similar bands were obtained from soluble *in vitro* Aβ aggregates corresponding to ADDLs (*23*, *24*) and protofibrils (*22*). Most studies have found that these oligomers are far more prevalent with Aβ(1−42) than with Aβ(1−40) (but see ref *25*). We examined aggregates formed from Aβ(1−40) and Aβ(1−42) monomers by SDS-PAGE and reached a similar conclusion (Figure 1). With relatively low loads (20 pmol) of monomeric Aβ taken immediately after SEC isolation, only 4 kDa monomer bands were apparent. After 1 day of incubation at 37 °C, the Aβ(1−42) sample showed substantial bands at 8−14 kDa that are generally referred to as dimers, trimers, and/or tetramers (here denoted 2−4mers) and a very broad band from 30 to 200 kDa. Most of the aggregates that give rise to these bands remained in the supernatant following centrifugation at 18000*g* (Figure 1) and thus may be considered soluble. Continued aggregation of this Aβ(1−42) sample for 7 days resulted in the disappearance of most of the 2−4mer bands. More of the aggregates were sedimented after 7 days, but substantial amounts remained soluble. Aggregates formed by Aβ(1−40) did not show similar bands on SDS-PAGE. After 3 days of incubation at 37 °C, most of the Aβ(1−40) was sedimented and only bands of $>$200 kDa along with monomer were observed.

Oligomers Corresponding to 2−4mers Coelute with Aβ(1−42) Monomers or Larger Aggregates during Size Exclusion Chromatography (SEC) and Are Minor Species in the Absence of SDS. The 2−4mer bands produced by Aβ(1−42) could reflect the formation of stable dimers, trimers, or tetramers during the 37 °C incubation, or they could be

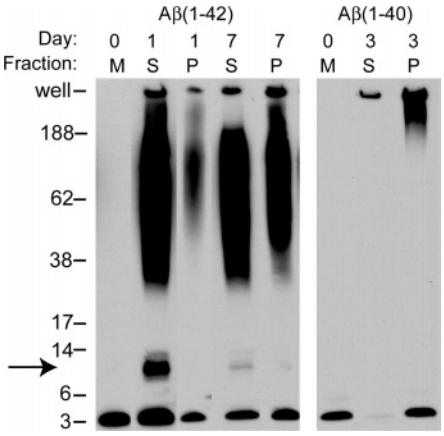

FIGURE 1: Analyses of Aβ(1−40) and Aβ(1−42) aggregation reactions by SDS-PAGE. Monomeric Aβ(1−40) and Aβ(1−42) (50 μM) were incubated in 150 mM NaCl, 20 mM Tris-HCl (pH 8.0) at 37 °C. At the indicated times, 50 μL aliquots were centrifuged (18000*g* for 10 min) to separate supernatant (S) and pellet (P) fractions, and 8% of each fraction was taken for SDS-PAGE and immunoblotting with monoclonal antibody 6E10. All samples were run on SDS-PAGE immediately after the incubation period. Samples of freshly isolated monomeric Aβ stocks (M, 20 pmol) were included for comparison. Bands corresponding to 2−4mers are indicated by the arrow.

generated from either monomers or larger aggregates by the action of SDS prior to PAGE. To address this question, we conducted a size analysis of two samples by SEC on a Superdex 75 column. The first sample consisted of monomeric Aβ(1−42), and to ensure the absence of aggregates we conducted a second cycle of SEC on the peak fractions from the initial monomer purification (Figure 2A). Our goal was to determine whether 2−4mer bands eluted from the column as species distinct from monomer. If this were the case, their elution volume should be shifted relative to that of monomer and ratios of 2−4mer to monomer bands should vary continuously among adjacent fractions. Immunoblot analysis with larger amounts of Aβ(1−42) (Figure 2C) showed 2−4mer bands only in peak monomer fractions, but this technique cannot resolve a quantitative shift in band ratios. To quantify these ratios, we extracted Aβ(1−42) from slices of gels run in triplicate with the gel in Figure 2C and measured the peptide in an ELISA assay. As shown in Figure 2E, the ratio of Aβ(1−42) in the 2−4mer bands to that in the monomer band was constant at about 0.06 across the five peak SEC fractions in Figure 2C. Therefore, we conclude that the 2−4mer bands do not reflect a stable species distinct from monomer in freshly isolated Aβ(1−42).

The second sample analyzed by SEC corresponded to an Aβ(1−42) aggregate mixture very similar to that obtained after the 1-day incubation in Figure 1. The immunoblot of column fractions showed 2−4mer bands along with intense 30 to >200 kDa bands and minor monomer bands at the void volume in fractions 16−18 (Figure 2D). Monomer bands were also observed in the residual monomer peak in fractions 29−31. ELISA measurement of Aβ(1−42) in the gel slices revealed a higher ratio of Aβ(1−42) in the 2−4mer bands to that in the monomer band (0.7) across the three peak void volume fractions (Figure 2F), an indication that most of these 2−4mer bands arose from dissociation of the larger aggregates during SDS-PAGE. ELISA measurements were also made of the ratio of Aβ(1−42) in the 2−4mer

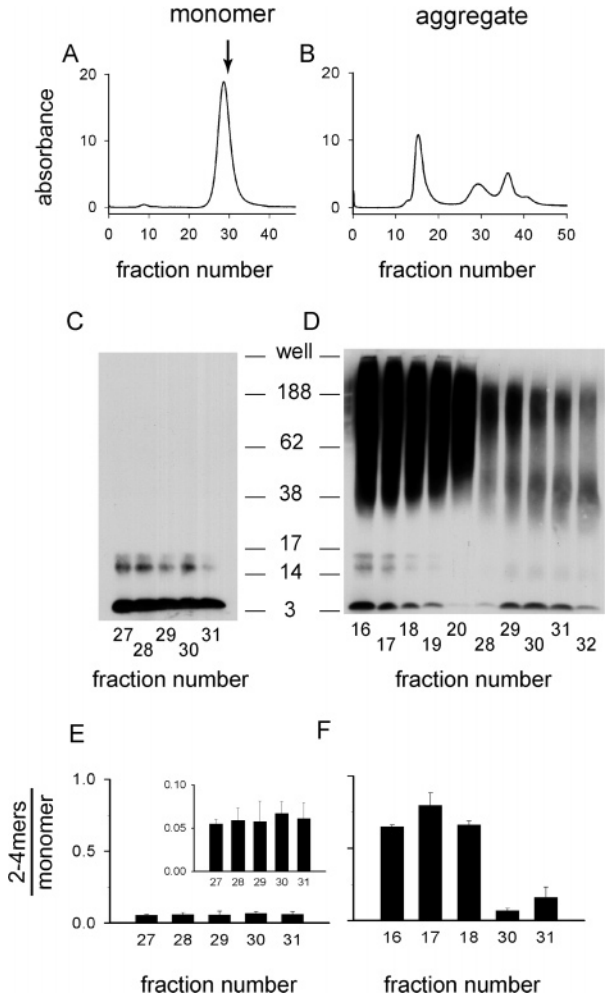

FIGURE 2: Coelution of 2−4mers with monomers or higher aggregates during SEC. Monomeric Aβ(1−42) was either immediately reapplied to the Superdex 75 column for another cycle of SEC (Panel A) or incubated as in Figure 1 for 16 h prior to loading the supernatant following centrifugation at 18000*g* on Superdex 75 (Panel B). Column elutions were monitored by the absorbance at 254 nm. The elution volume of Aβ(1−42) was just slightly larger than that of cytochrome *c* (12.5 kDa, arrow in Panel A), but cytochrome *c* as a globular protein does not provide an accurate calibration of monomeric Aβ(1−42), which is a random coil (*39*, *40*). C, D) Selected fractions were run on SDS-PAGE and immunoblotted as in Figure 1. In panel C, fractions were diluted to 10 μM Aβ(1−42) in 20 mM Tris-HCl and 180 pmol were loaded. In panel D, 15−20 pmol were loaded from fractions 16−18, 30, and 31, and smaller amounts (in maximum 20 μL volumes) from the remaining fractions. E, F) Selected fractions were run on SDS-PAGE, and gels were sliced and Aβ bands extracted for ELISA measurements of monomers, 2−4mers, and 15−200 kDa aggregates as outlined in the Experimental Procedures. Fractions in panel E correspond to the monomer fractionation in panels A and C, and those in panel F are from the aggregate fractionation in panels B and D. The inset in panel E shows the panel E data on a more sensitive scale. Averages are from triplicate gels run in parallel. Aβ amounts loaded were identical to those in panels C and D. Ratios in panel E were independent of sample load with samples up to 25 μM but increased about 3-fold when a small aliquot of concentrated sample buffer was diluted into 50 μM Aβ(1−42) and 500 pmol was loaded (data not shown).

bands to that in the 30 to >200 kDa band in fractions 16−18. This ratio (0.6) appeared relatively high based on the intensity of bands in the immunoblot in Figure 2D, suggesting either that the 30 to >200 kDa band was stained more intensely by antibody 6E10 or that the efficiency of

dissociation and extraction of Aβ(1−42) from the 30 to >200 kDa band may have been lower than that of the 2−4mer and monomer bands. However, regardless of this relative efficiency, the fact that the ratio of 0.6 was also constant across the three void volume fractions supported the conclusion that the 2−4mer bands resulted from dissociation of the larger aggregates. ELISA measurements also detected Aβ(1−42) in 2−4mer bands in the monomer peak (fractions 30 and 31) in Figure 2D. The ratio of Aβ(1−42) in these bands to that in the monomer band was again about 0.1 (Figure 2F), indicating that these 2−4mer bands also were generated from the residual monomer in the sample.

Figure 2A also shows additional UV absorbance in fractions 36−40 which is comparable to that in the monomer peak in fractions 29−31. The source of this absorbance is unclear. Fractions 36−40 showed no UV maximum at 276 nm, in contrast to the monomer peak, and less than 10% of the peptide content of the monomer peak by BCA assay.

SDS Concentrations Far below the Critical Micelle Concentration Accelerate the Aggregation of Aβ(1−42). The SEC results in Figures 2A and 2C indicate that 2−4mer bands do not elute as distinct pre-existing species in the absence of SDS but are generated from Aβ(1−42) monomer by the introduction of SDS. To examine this process in greater detail, we incubated Aβ(1−42) at various concentrations of SDS and compared the results to our recent study (*28*) of Aβ(1−40) aggregation in SDS. The aggregation of Aβ peptides was conveniently monitored by fluorescence with thioflavin T. This fluorophore shows greatly enhanced fluorescence upon binding to amyloid fibrils (*35*), Aβ protofibrils (*31*, *42*), and certain other Aβ aggregates enriched in β-structure (*39*). Rates of aggregation with 25 μM concentrations of Aβ(1−40) and Aβ(1−42) were compared in the presence and absence of SDS (Figure 3). Without SDS, Aβ(1−42) aggregated after a delay or lag time of 56 h, while Aβ(1−40) failed to aggregate over the observed 10-day time interval (Figure 3A and B). These observations are consistent with previous reports that Aβ(1−42) aggregates more rapidly than Aβ(1−40) (*22*, *43*). EM of the Aβ(1−42) sample revealed filamentous structures (Figure 4A) which resembled Aβ(1−40) protofibrils that had been elongated by monomer deposition while remaining largely soluble following centrifugation at 18000*g* (*31*). Under the salt conditions in Figure 3, the Aβ(1−42) aggregates that gave thioflavin T fluorescence also remained soluble.

Addition of SDS resulted in accelerated Aβ(1−40) aggregation but only over a narrow range of SDS concentrations. A maximal rate of Aβ(1−40) aggregation was observed in 2 mM SDS (Figures 3A and C), a concentration near the critical micelle concentration (CMC) for SDS under the buffer conditions employed (*28*). We previously concluded that the aggregation was accelerated because a high ratio of Aβ peptides to small SDS micelles facilitated a close proximity of peptides on micelle surfaces and thereby promoted intermolecular association (*28*).

Aggregation of Aβ(1−42) also was accelerated over a narrow range of SDS concentrations, but the maximal rate was observed with only 0.5 mM SDS (Figures 3B and 3D). This aggregation progressed quickly without a significant lag-time, and the fluorescence remained high over the remaining 10-day incubation period (Figure 3B). A previous report also found that aggregation of Aβ(1−40) and Aβ(1−42) as measured by thioflavin T fluorescence was promoted by optimal concentrations of SDS similar to those in Figure 3 (*27*). A proximity effect like the one we proposed for Aβ(1−40) in 2 mM SDS could explain a maximal rate of Aβ(1−42) aggregation in 0.5 mM SDS, if Aβ(1−42) promoted SDS micelle formation more strongly than Aβ(1−40). However, it was surprising that, in contrast to Aβ(1−40), Aβ(1−42) in 2 mM SDS gave little or no increase in thioflavin T fluorescence (Figure 3B and 3D). Examination of this reaction by EM after 172 h revealed a few amorphous

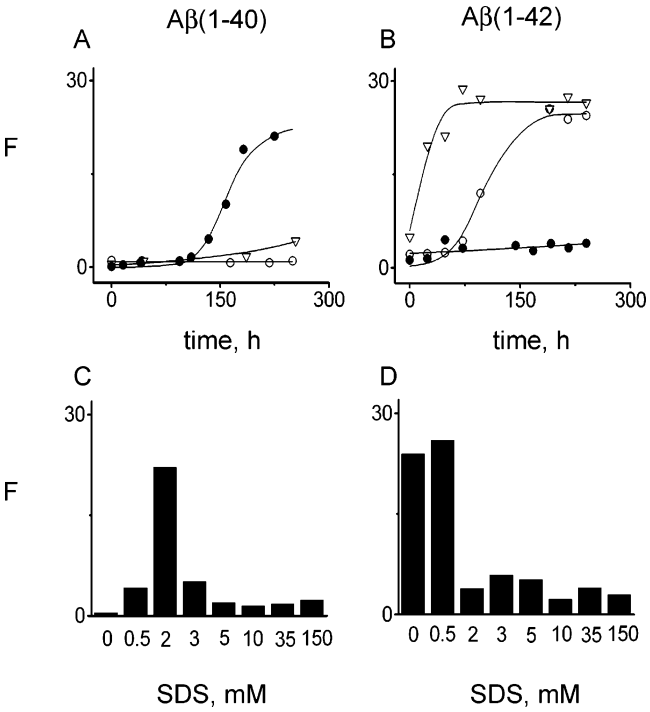

FIGURE 3: Dependence of Aβ(1−40) and Aβ(1−42) aggregation on the SDS concentration as monitored by thioflavin T fluorescence. Monomeric Aβ(1−40) (Panel A) or Aβ(1−42) (Panel B) (25 μM) was incubated in buffer (5 mM Tris-HCl, 50 mM NaCl, pH 8.0) alone (○) or with 0.5 mM SDS (▽) or 2.0 mM SDS (●, data from reference (*28*)). At the indicated times, aliquots were diluted 15-fold for measurement of thioflavin T fluorescence. Values of F were fit to eq 1 (solid lines) to give lag times of 125 ± 4 h for points ● in Panel A and of <1 h and 56 ± 4 h for points ▽ and ○, respectively, in Panel B. Fluorescence intensities at ∼240 h for Aβ(1−40) (Panel C) or Aβ(1−42) (Panel D) were taken from Panels A and B as well as from additional reactions run in parallel at the indicated SDS concentrations.

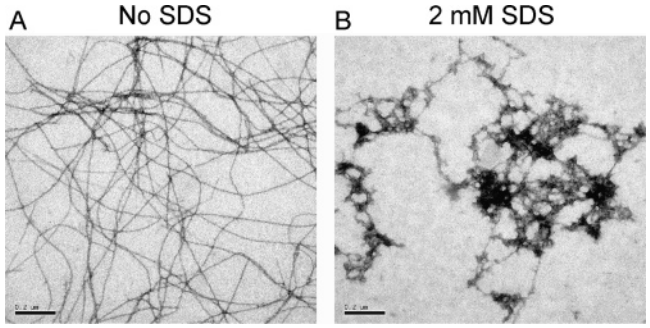

FIGURE 4: Electron micrographs of Aβ(1−42) aggregates formed without SDS and with 2 mM SDS. Aliquots (10 μL) from the reaction mixtures with 25 μM Aβ(1−42) without SDS (panel A) or with 2 mM SDS (panel B) in Figure 3 were removed after 172 h and processed for negative staining and EM. Images are shown relative to a calibration bar of 200 nm.

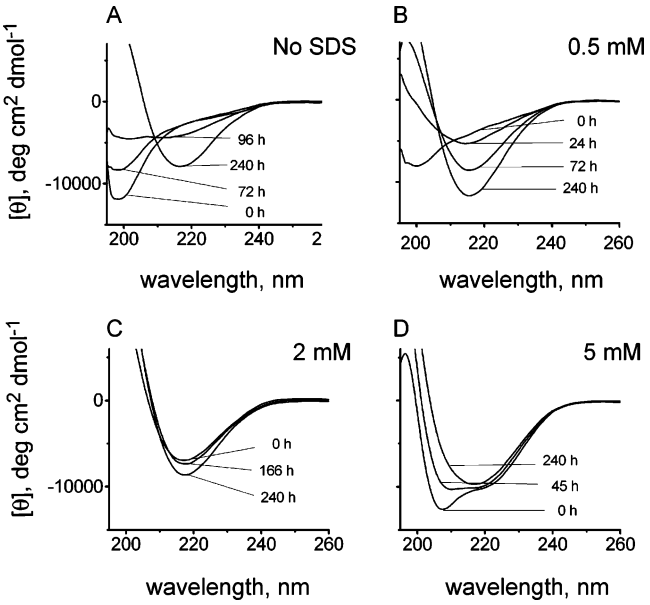

FIGURE 5: Secondary structure changes indicated by far-UV CD during aggregation of Aβ(1−42) with or without low concentrations of SDS. Aliquots of reactions with 25 μM Aβ(1−42) in Figure 3 were transferred at various times to a CD cuvette, and spectra were recorded. Representative spectra are shown for the Aβ(1−42) samples taken at the indicated times in the absence of SDS (Panel A) and in 0.5 mM (Panel B), 2 mM (Panel C), and 5 mM SDS (Panel D).

structures in a loose lattice (Figure 4B) but no filaments like those in Figure 4A. With SDS concentrations at or slightly above 3 mM, 10-day incubations of Aβ(1−42) as well as Aβ(1−40) resulted in fluorescence that was marginally higher than the background but far lower than that at the optimum SDS concentrations (Figures 3C and 3D).

Secondary Structure Changes of Aβ(1−42) during Aggregation in SDS. To obtain further information about the structural changes in Aβ(1−42) that occur during incubation in various concentrations of SDS, we periodically took aliquots from reactions represented in Figure 3D and obtained circular dichroism (CD) spectra. At SDS concentrations well above the CMC (10, 35 and 150 mM), Aβ(1−42) exhibited CD spectra consistent with a largely α-helical conformation, with minima near 208 and 222 nm (data not shown). These spectra remained unchanged over the 10-day incubation period and were similar to CD spectra obtained in high concentrations of SDS with Aβ(1−40) (*28*) and many other proteins (*44*−*47*). An abundance of SDS micelles at these high concentrations virtually eliminates intermolecular interaction of Aβ peptides on the surface of a single micelle, and individual peptides are stabilized by the micelles predominantly as α-helices. In contrast, CD spectra at lower SDS concentrations or without SDS revealed time-dependent changes in Aβ conformation. Spectra for Aβ(1−42) in the absence of SDS (Figure 5A) as well as in 0.5 mM SDS (Figure 5B) initially showed no minima above 200 nm and were consistent with previous reports on Aβ(1−40) (*28*, *48*) and Aβ(1−42) (*49*) of a largely random coil conformation in aqueous buffers prior to aggregation. Both of these samples showed progressive conversion to a predominant β-structure, characterized by a negative minimum at 218 nm, over the 10-day incubation period. The emergence of β-structure in both samples correlated with the increases in thioflavin T fluorescence shown in Figure 3B. This trend is consistent with our previous demonstration of a close correlation between the slow conversion to β-structure by CD and the increase in thioflavin T fluorescence for Aβ(1−40) in 2 mM SDS (*28*). In sharp contrast, addition of 2 mM SDS to Aβ(1−42) resulted in an immediate appearance of β-structure, and the shape of the spectra remained unchanged for ∼240 h with only a marginal increase in the mean residue ellipticity (Figure 5C). Since this sample failed to show significant thioflavin T fluorescence throughout the entire 10-day incubation (Figure 3B), we conclude that Aβ(1−42) in 2 mM SDS forms β-structured aggregates that differ from those generated in 0.5 mM SDS or in the absence of SDS. CD spectra of Aβ(1−42) in 3 mM (data not shown) and 5 mM SDS (Figure 5D) initially showed a predominant α-helical conformation (0 h curve) that gradually converted to a β-structure. These spectral changes resembled those observed during incubation of Aβ(1−40) in 2 mM SDS (*28*), but the changes with Aβ(1−40) were accompanied by a corresponding increase in thioflavin T fluorescence whereas those with Aβ(1−42) were not. The hydrophobicity introduced by the two additional amino acids (Ile-Ala) at the C-terminus of Aβ(1−42) may induce a qualitatively different peptide alignment on dilute SDS micelles that results in an alternative β-structured aggregate. A conversion from α-helical to β-structure was also observed when amylin (IAPP) was incubated with DOPG liposomes and, as with Aβ(1−40), the time scale of the conversion was consistent with measurements of fiber formation by thioflavin T fluorescence (*50*). There also appeared to be a quantitative difference in the extent of β-structure formation by Aβ(1−42) in 2, 3, and 5 mM SDS, as the mean residue ellipticity values at 218 nm (characteristic of β-structure) remained at ∼8000 deg cm^2 dmol^{-1} and never exceeded this intensity, while those with 0.5 mM SDS saturated at ∼12000 deg cm^2 dmol^{-1} (Figure 5).

Progressive Formation of Aβ(1−42) Oligomers in 2 mM SDS. In view of the unexpected increase in β-structure in the absence of thioflavin T fluorescence when Aβ(1−42) is incubated in 2 mM SDS, SDS-PAGE analyses were conducted to investigate changes in the state of Aβ(1−42) aggregation. With 25 μM Aβ(1−42) in 2 mM SDS, only a monomeric Aβ band was initially observed, but first 2−4mer bands and then bands near 40 kDa became apparent. The time course of this progression varied somewhat from sample to sample. In Figure 6A, a significant monomer band remained after 1 h and virtually all of the Aβ was localized in 2−4mer bands with only a faint band near 40 kDa after 24 h. In other samples, most Aβ was found in 2−4mer bands within 0.5 h (see Figure 7A). In all cases, however, while the conversion to a predominant β-structure by CD was nearly complete within the roughly 5 min required for the initial spectrum measurement (Figure 5C), the complete loss of the monomer band on SDS-PAGE gels required considerably more time. Therefore, the change in conformation precedes the formation of oligomers that can be detected by SDS-PAGE.

Barghorn and co-workers (*26*) recently reported the isolation of a stable Aβ(1−42) oligomer that migrated as a doublet of 38 and 48 kDa bands on SDS-PAGE. This oligomer, which they called a 38/48 kDa "globulomer", was generated in a multistep procedure that involved initial 6-h incubation in 7 mM SDS, subsequent 16-h incubation at

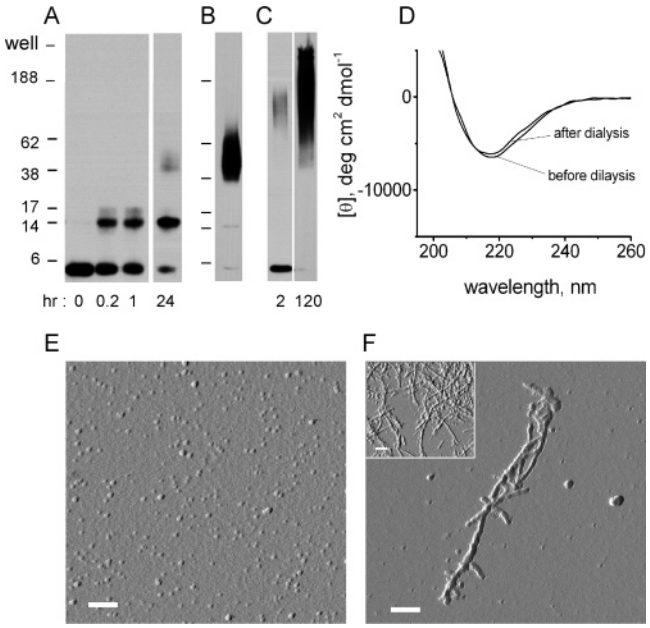

FIGURE 6: Aβ(1−42) oligomers are formed in high yield in 2 mM SDS and are distinct from fibrils. (A) Parallel samples of monomeric Aβ(1−42) (25 μM) were incubated in 20 mM Tris-HCl, 50 mM NaCl (pH 8.0) with 2 mM SDS for the indicated times. The 0-, 0.2-, and 1-h incubations were staggered so that each sample (10 pmol) was subjected to SDS-PAGE immediately after incubation. LDS (2 mM) was substituted for 1% LDS in the sample loading buffer to minimize potential oligomer dissociation, but this substitution had little effect on banding patterns. (B) After 24-h incubation of Aβ(1−42) as in panel A, the sample was dialyzed using a 25000 MWCO dialysis membrane (Spectra/Por) for 48 h against 10 mM Tris-HCl (pH 8.0) in the absence of SDS and centrifuged (18000*g* for 10 min). An aliquot (8 pmol) of the supernatant was transferred to 1% LDS loading buffer and run on SDS-PAGE. (C) Monomeric Aβ(1−42) (50 μM) was incubated in buffer containing NaCl at 37 °C as in Figure 1 for the indicated times, and aliquots (10 pmol) were transferred to 1% LDS loading buffer and run on SDS-PAGE. Gels from panels A−C were immunoblotted, and blots were stained with antibody 6E10. (D) CD spectra of the 24-h sample in panel A and the dialyzed sample in panel B. (E, F) Atomic force microscopy (AFM) of the sample in panel B and the 120-h sample in panel C, respectively. Aliquots were diluted with 100-fold with water, and 150 μL was applied to mica disks. The average height was 1.9 ± 0.7 nm (SD, n = 447) for globular particles including those in panel E, and the range of heights was 3−9 nm for the fibrils in panel F. Images, shown in amplitude mode, are 1 × 1 μm and calibration bars are 100 nm. The inset in panel F also is 1 × 1 μm.

1.8 mM SDS at 37 °C, and final removal of SDS. Of particular note, the SDS-PAGE banding pattern of this globulomer was preserved after it was either extensively dialyzed or precipitated with cold methanol/acetic acid. The globulomer structure appeared to exist *in vivo*, as a monoclonal antibody generated to isolated globulomers cross-reacted at the periphery of amyloid plaques in the brains of AD patients. Since the SDS-PAGE profiles following our 24-h incubations of Aβ(1−42) in 2 mM SDS and their 16-h incubation showed banding patterns similar to globulomers, we examined the stability of our aggregates following dialysis. After removal of the SDS by dialysis of this sample for 48 h, SDS-PAGE analysis showed almost complete loss of the 2−4mer bands but a dramatic increase in the intensity of 30−60 kDa bands (Figure 6B), sometimes extending to >200 kDa. More than 80% of the Aβ(1−42) was recovered following dialysis, and virtually all of the dialyzed oligomers remained in the supernatant following centrifugation at 18000*g* for 10 min. The CD spectrum of the dialyzed sample (Figure 6D) showed a retention of β-structure with a mean residue ellipticity at 218 nm comparable to that of the initial aggregate produced in 2 mM SDS. Dialysis also resulted in small increases in fluorescence with thioflavin T, suggesting the formation of a few protofibrils and fibrils (data not shown). However, when the dialyzed sample was examined by atomic force microscopy (AFM), filamentous structures were difficult to find (Figure 6E). The AFM image showed globular species with an average height of 1.9 nm. Our initial attempts to isolate and characterize the dialyzed oligomers have been hindered by extremely low recoveries following SEC on Superdex-75.

We investigated whether the 2−4mers that predominate after 24-h incubation of Aβ(1−42) in 2 mM SDS also could be observed by AFM. Since the 2−4mers are stabilized by interaction with SDS micelles, we also examined a parallel sample of 25 μM Aβ(1−42) in 10 mM SDS, where Aβ(1−42) remains monomeric, as well as both SDS buffers as controls. No particles greater than 1 nm were detected in the buffers. Particles similar in appearance to those in Figure 6E were observed with Aβ(1−42), and a small difference in particle height was observed between Aβ(1−42) in 2 mM SDS (2.4 ± 1.0 nm (SD, n = 540)) and 10 mM SDS (1.8 ± 0.7 nm (SD, n = 469) data not shown). Thus, the heights of the 2−4mers associated with micelles in 2 mM SDS were slightly greater than those of the dialyzed oligomers in Figure 6E.

Incubation of 50 μM Aβ(1−42) in buffered 150 mM NaCl at 37 °C in the absence of SDS resulted in considerable aggregate formation within 1 day (Figure 1). To assess early intermediates and final products on this aggregation pathway, a similar reaction was initiated and monitored by thioflavin T fluorescence. Aggregation was in an early stage after 2 h, as the relative fluorescence was only about 4% of the final plateau value obtained after 48 h. After 120 h all of the aggregates that generated fluorescence were sedimented at 18000*g* for 10 min, and AFM confirmed that the sample at this point consisted of fibrils (Figure 6F). To determine whether 2−4mers are the initial aggregation intermediates under these conditions, the 2- and 120-h samples were subjected to SDS-PAGE. Most of the Aβ(1−42) migrated in the monomer band in the 2-h sample, but a broad but clear aggregate band was apparent at 100−120 kDa and no 2−4mer bands were detected (Figure 6C). After 120 h this band had broadened considerably but contained virtually all of the Aβ(1−42). Therefore, we conclude that 2−4mers are not detectable as initial intermediates on this fibril formation pathway.

Dissociation of Aβ(1−42) Aggregates following Boiling in 35 mM LDS. In our routine SDS-PAGE analyses, samples were not boiled in the 1% (35 mM) LDS loading buffer before SDS-PAGE electrophoresis. We examined the stabilities of several of the aggregates formed by Aβ(1−42) by comparing banding patterns with and without boiling the samples in the loading buffer prior to SDS-PAGE. In all cases, bands larger than the monomer band were abolished by boiling. These bands included the initial 2−4mers generated in 2 mM SDS (Figure 7A), the 30−60 kDa oligomer species formed after dialysis of the samples incubated in 2 mM SDS (Figure 7B), and high M_w bands

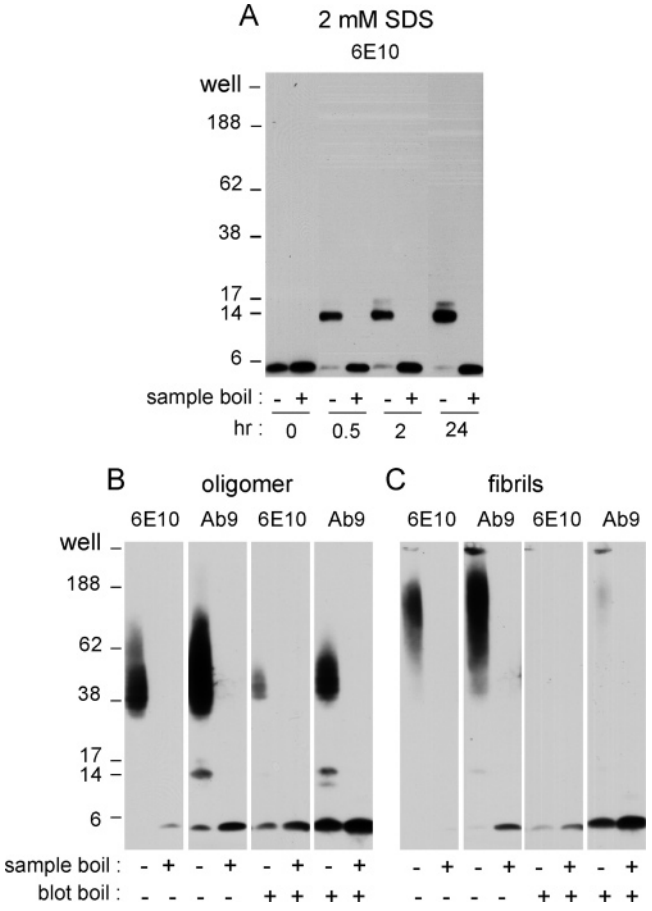

FIGURE 7: Thermal stability of Aβ(1−42) oligomers and fibrils determined by SDS-PAGE. Monomeric Aβ(1−42) was incubated in the presence or absence of 2 mM SDS as in Figure 6, and samples (10 pmol) were transferred to 1% LDS sample buffer and either maintained at 25 °C or boiled for 5 min before analysis by SDS-PAGE. (A) Samples in 2 mM SDS for the indicated times. (B) Samples in 2 mM SDS for 24 h followed by dialysis for 48 h. (C) Samples in Tris-HCl-buffered NaCl for 120 h. In panels B and C, parallel blots were either boiled or left unboiled (see Experimental Procedures) before immunostaining either with antibody 6E10 or Ab9 as indicated.

obtained from fibrils generated during incubation of Aβ(1−42) in 150 mM NaCl at 37 °C (Figure 7C). Monomer band intensities on immunoblots stained with antibody 6E10 increased following boiling of the dialyzed oligomer and the fibril samples, but the increase in these intensities was considerably less than the intensities of the higher M_w bands in the samples that were not boiled. This difference appeared simply to be a technical issue. Immunoblotting with antibody Ab9 gave greater intensities in monomer bands after sample boiling (Figures 7B and 7C). Furthermore, Aβ monomer band intensities were reported to be enhanced by boiling blots prior to immunostaining (*14*), and this treatment further increased the intensities of monomer bands but strikingly decreased the intensities of bands >30 kDa with both 6E10 and Ab9 (Figures 7B and 7C). The ELISA analysis in Figures 2E and 2F was applied to extracted gel slices corresponding to monomer bands from the oligomer sample in Figure 7B. In agreement with apparent monomer intensities from the boiled blots in Figure 7B, sample boiling was found to double the level of extracted monomer. This observation was consistent with a complete transfer of Aβ in aggregate bands to monomer bands following sample boiling in LDS loading buffer. The key point, however, is that SDS-PAGE bands corresponding to our *in vitro* oligomers were completely abolished by boiling in SDS. In sharp contrast, endogenous oligomer samples appear to be routinely boiled in sample buffer containing 1−2% SDS in preparation for SDS-PAGE without disruption of the oligomer gel bands (*13*, *14*, *16*, *19*).

DISCUSSION

Distinctions between Endogenous Aβ Oligomers and Aβ Oligomers Generated in Vitro. The hypothesis that soluble oligomeric aggregates of Aβ are the principal toxic species leading to AD has been strengthened by recent progress in the biochemical fractionation of these aggregates. In particular, SEC of conditioned medium from cultured cells or of brain extracts from transgenic mice has allowed separation of Aβ oligomers from both Aβ monomers and large Aβ aggregates. Multiple Aβ bands of 6 to 14 kDa were detected by SDS-PAGE in samples of Aβ immunoprecipitated from the conditioned medium of CHO cells that had been transfected with APP cDNA (*16*), and these apparent Aβ dimers and trimers were separated by SEC on Superdex 75 in buffers without SDS (*13*, *19*). Fractions containing the dimers and trimers but not Aβ monomers inhibited hippocampal long-term potentiation. Transgenic Tg2576 mice express a mutant human APP that generates substantial Aβ levels (*18*). Brain extracts from Tg2576 mice, but not nontransgenic littermates, contained apparent Aβ trimers as well as oligomers that migrated as multiples of trimers on SDS-PAGE, and these oligomers were also separated by SEC on Superdex 75 (*14*). Among these oligomers, the levels of an apparent dodecamer denoted Aβ*56 correlated best with spatial memory deficits exhibited by the transgenic mice. When Aβ*56 was purified by immunoprecipitation, separated from other Aβ oligomers by SEC, and infused into the lateral ventricles of the brains of young rats, it impaired the retention of spatial memory (*14*).

These demonstrations of deficits in neuronal function and memory retention highlight the importance of better defining the structures of Aβ oligomers as potential therapeutic targets. However, the low levels of the endogenous oligomers make such a characterization extremely difficult. A reasonable alternative is to reconstitute Aβ oligomers from chemically synthesized Aβ *in vitro*. Initial observations of *in vitro* oligomer formation have been encouraging. Aβ 2−4mers that resemble the endogenous dimers, trimers, and tetramers are readily detected when Aβ(1−42) is incubated, and higher levels of 2−4mers are formed from Aβ(1−42) than from Aβ(1−40) (Figure 1). Since mutations that increase the ratio of Aβ(1−42) to Aβ(1−40) lead to FAD (*6*), this trend suggests a basis for the greater toxicity of Aβ(1−42). In addition, a broad band of oligomers in the 35−200 kDa region are obtained during incubation of Aβ(1−42) (Figure 1). While not exhibiting as sharply discrete SDS-PAGE bands as the endogenous Aβ oligomers reported by Lesne et al. (*14*), they nevertheless span a similar size range. However, the similarities break down when elution patterns from SEC are compared. Fractionation of monomeric or aggregated Aβ(1−42) generated *in vitro* by SEC fails to resolve stable 2−4mers (Figures 2 and 3), in contrast to the well-resolved profiles obtained with the endogenous oligomers.

One possible explanation for the difference in stability between endogenous Aβ oligomers and oligomers prepared *in vitro* is a fundamental divergence in aggregate structure. Cellular interfaces may serve as templates for structures that cannot readily be formed in aqueous buffers *in vitro*, and there is strong evidence for interactions between endogenous Aβ and cell membranes. Sphingolipid- and cholesterol-rich bilayer membranes known as lipid rafts (*51*) are enriched in the β- and γ-secretases that generate Aβ peptides from APP as well as in the Aβ peptides themselves (*52*−*54*). In Tg2576 transgenic mice, Aβ was highly concentrated in lipid rafts in a form that corresponded almost exclusively to dimeric bands on SDS-PAGE gels (*12*). Some of these interactions may occur at similar membrane interfaces *in vitro*. Several reports have shown that anionic micelles composed of gangliosides as well as reconstituted liposomes that resemble lipid rafts promote Aβ binding and β-structure formation (*55*−*58*). We have explored the features of interfaces responsible for these effects and found that both polar−nonpolar interfaces (*39*, *59*) and anionic micelles formed by SDS (*28*) induce Aβ aggregation. In particular, dilute anionic micelles formed in 2 mM SDS promote the formation of soluble fibers by Aβ(1−40) (Figure 3A,C and ref *28*) and of soluble oligomers and globulomers by Aβ(1−42) (Figures 4, 7 and ref *26*). However, the introduction of SDS micelles did not result in the formation of more stable Aβ(1−42) oligomers. Fractionation of Aβ(1−42) samples incubated in 2 mM SDS by SEC in detergent-free buffer resulted in complete dissaggregation to monomers (data not shown). Therefore, introduction of this anionic micellar interface alone is not sufficient to generate Aβ(1−42) oligomers that can be resolved as stable discrete species by SEC.

Differences between endogenous Aβ oligomers and oligomers prepared *in vitro* are also shown by their thermal stabilities. Endogenous oligomer samples appear to be routinely boiled in sample buffer containing 1−2% SDS in preparation for SDS-PAGE without disruption of the oligomer gel bands (*13*, *14*, *16*, *19*). However, comparable amounts of *in vitro* Aβ aggregates completely dissociate to monomers when boiled in SDS (Figure 7). This difference may not be fully appreciated from previous reports because early studies of Aβ(x-43) (*41*) and Aβ(1−42) (*21*, *22*) reported trimer and tetramer bands on SDS-PAGE gels even when the samples were boiled in SDS just before electrophoresis. The key issue here appears to be the quantity of peptide in the samples. Nanomolar amounts of peptides were loaded on the gels in these early studies to allow detection with standard protein stains, in contrast to the 10−180 pmol loads in our immunoblots, and with our ELISA assay we observed an increase in the ratio of 2−4mer to monomer with a 500 pmol load (see legend to Figure 2). In a more recent report in which Aβ oligomers were detected by immunoblotting, SDS-PAGE sample onputs were not heated before electrophoresis (*25*). Other amyloids also appear susceptible to boiling. Fibrils formed by the NM domain of the yeast prion protein Sup35 exhibited high M_W aggregates on agarose gel electrophoresis following treatment with 1−2% SDS at room temperature but were completely disaggregated by a 7-min treatment with 1−2% SDS at 95 °C (*60*).

Since the endogenous Aβ oligomer bands were observed even after boiling in 1−2% SDS whereas the Aβ oligomers and protofibrils generated from synthetic Aβ *in vitro* were not, it is important to consider whether the endogenous oligomers were covalently cross-linked in their cellular environments. Lesne et al. (*14*) addressed this point by treating their Tg2576 brain extracts with HFIP, a popular solvent for solubilizing peptides and proteins (*61*), prior to SDS-PAGE. They observed a loss of Aβ oligomers greater than trimers and an increase in monomers when the HFIP concentration was more than 10%, but the trimer bands persisted to 45% HFIP. In data not shown, the trimer band was said to dissociate to monomers with >55% HFIP. Although this data suggests that the endogenous oligomers were not cross-linked (*14*), this issue should be examined with other techniques. Several agents have been shown to generate Aβ oligomers *in vitro* that are stable to boiling in SDS, presumably by promoting covalent intermolecular cross-linking. These include Cu^{2+} (*62*, *63*), transglutaminase (*64*, *65*), and prostaglandin products of cyclooxygenase (*66*, *67*). These cross-linking agents also could be important in a physiological context, particularly if they were concentrated near cellular interfaces that promoted Aβ aggregation.

Effects of SDS on Aβ(1−42) Conformation and Aggregation. In our previous study (*28*), we concluded that micelles formed in dilute SDS (2 mM) promote fiber formation by Aβ(1−40) because they support peptide interaction on the surface of a single micelle complex. A similar promotion of amylin fiber formation was observed with DOPG liposomes (*50*). Here we show that this process may occur with Aβ-(1−42) in even more dilute SDS (0.5 mM). However, Aβ-(1−42) but not Aβ(1−40) exhibits an additional aggregation process in 2 mM SDS that results in conversion of most of the peptide to 2−4mers within a day (Figure 6A) followed by slower conversion to larger aggregates in the 35−200 kDa range. These larger aggregates are stable enough to largely resist dissociation during removal of SDS by dialysis (Figure 6B).

It has been argued that SDS-PAGE is not a useful method for identification and quantitation of noncovalently associated protein oligomers because SDS can induce artificial oligomerization (*68*). Our data here reinforce the point that SDS can induce oligomerization, but this induction can be largely avoided in conventional SDS-PAGE analyses with appropriate precautions. Incubation of monomeric Aβ(1−42) at concentrations of SDS below about 0.1−0.2% can generate oligomer bands on SDS-PAGE, but this conversion is not instantaneous. When 2 mM SDS is added to freshly isolated monomeric Aβ(1−42) and the sample is immediately subjected to SDS-PAGE, oligomer bands are below limits of detection even when the gel running buffer also contains 2 mM SDS (Figure 6A). Bands corresponding to 2−4mers become apparent within 10 min of incubation in 2 mM SDS (Figure 6A), and the rate at which these bands appear increases at higher concentrations of Aβ(1−42) (data not shown). Once oligomers are formed, they resist dissociation in 1% SDS loading buffers unless the sample is heated (Figure 7). CD spectra of Aβ(1−42) indicate that conversion to nearly the final extent of β-structure occurs as soon after addition of 2 mM SDS as a spectrum can be recorded (Figure 5C). This indicates that the conformation Aβ(1−42) monomers is immediately altered to that characteristic of oligomers by interaction with micelles in 2 mM SDS, but that oligomers

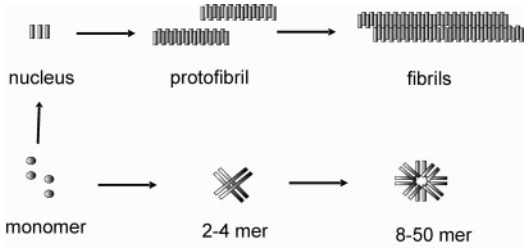

FIGURE 8: Two alternative pathways of Aβ aggregation. The nucleation-dependent pathway (upper) includes protofibril intermediates and leads to fibril formation. A second pathway (lower) involves soluble oligomer formation (2−4 mers and 8−50mers). These oligomers proceed on to mature fibrils slowly if at all.

stable enough to detect on SDS-PAGE take somewhat longer to form.

When concentrated SDS-PAGE sample buffer is diluted directly into monomeric Aβ(1−42), the relative level of 2−4mer bands depends on the peptide concentration. With concentrations below 25 μM, the level of 2−4mer bands is about 6% of that of the monomer band (Figure 2E). One possible explanation for the appearance of these 2−4mer bands starts with the premise that Aβ(1−42) monomers in detergent-free buffers are in rapid equilibrium with small oligomers. Such an equilibrium has been inferred from oligomer banding patterns following rapid cross-linking with a PICUP procedure (*69*). If 1% LDS is able to trap these oligomers as stabilized species that do not equilibrate with monomers during SDS-PAGE, discrete oligomer bands would be evident. An alternative possible explanation for the 2−4mer bands considers the dilution of SDS during conventional SDS-PAGE. Monomers that interact with the micelles in 1% LDS and assume a predominant α-helical conformation do not aggregate at a significant rate. During electrophoretic migration of the sample into gel running buffer containing 0.1% SDS, however, monomers may encounter an SDS concentration sufficient to initiate a conversion to β-structure (Figures 5 C and D) and subsequent oligomerization (Figure 6A). We have confirmed by CD that dilution of Aβ(1−42) monomers from 1% SDS to 0.1% SDS results in the same extent of β-structure as when monomers are added directly to 0.1% SDS and on a time scale well within the 2−3 h required for a typical SDS-PAGE run. This explanation may be a little less likely because it should result in gradual oligomerization and more diffuse bands than are observed. Such considerations aside, however, the question of how to interpret oligomer bands obtained from Aβ(1−42) incubations added directly to SDS-PAGE sample buffers remains. Our data suggest that, if these bands are well in excess of the relatively low levels obtained from purified monomer samples run in parallel, they are likely to reflect aggregates that existed before contact with SDS.

Alternative Aβ Aggregation Pathways. Aβ fibril formation *in vitro* is thought to involve nucleation-dependent polymerization (*22*, *43*). In this process, monomeric Aβ associates noncovalently to form nuclei or "seeds", which then grow into soluble protofibrils and insoluble fibrils (as represented by the upper pathway in Figure 8). Nucleus formation is considered rate-limiting in this process, but the low level of any putative nucleus species has made its biochemical detection extremely difficult. Evidence for this pathway largely is provided by two widespread observations: protofibril formation from monomers proceeds with a lag phase prior to the onset of aggregation (see Figure 3A and 3B), and small amounts of protofibrils or fibrils act as seeds when added to monomers to eliminate the lag phase. Protofibrils are formed by both Aβ(1−40) and Aβ(1−42) and can be isolated by SEC (*22*, *31*). They exhibit Stokes radii of 10−50 nm as measured by dynamic light scattering (*22*), show enhanced fluorescence with thioflavin T (*31*, *42*) (although see (*70*)), give circular dichroism (CD) spectra that reveal β-structure (*42*), and display mixtures of roughly spherical globules, short, curly fibers (*22*, *37*, *71*) and short rods of 10−200 nm (*31*, *72*−*74*) by electron microscopy (EM) and atomic force microscopy (AFM). An alternative process (represented by the lower pathway in Figure 8) involves the initial formation of small oligomers that become progressively larger with longer incubation. Models of alternative pathways with similar features were recently proposed by two groups (*26*, *75*). The small oligomers are represented by the 2−4mers observed on SDS-PAGE, but their actual size prior to contact with SDS is unclear. While these oligomers remain minor species during Aβ(1−42) incubation in the absence of detergent, this pathway emerges as an alternative to fibril formation because it is strongly promoted by 2 mM SDS and perhaps by dilute anionic micelles in general. In support of this argument, Aβ(1−42) was immediately converted to a predominant β-structure conformation in 2 mM SDS (Figure 5C), and progressive conversion of virtually all monomers to 2−4mers and higher oligomers in 2 mM SDS was essentially complete within a day (Figure 6A). However, this aggregation did not lead to more rapid fibril formation. Continued incubation of 25 μM Aβ(1−42) in 2 mM SDS gave no increase in fluorescence with thioflavin T and no appearance of fibrils by EM, in contrast to parallel incubations in the absence of SDS that resulted in both thioflavin T fluorescence and fibril formation (Figures 3B and 4). Oligomers represented by 38−48 kDa bands extending to 200 kDa remained stable following removal of the 2 mM SDS by dialysis and closely resembled the globulomer preparation described previously (*26*). An increase in thioflavin T fluorescence following dialysis indicated some protofibril formation during dialysis, but there was no evidence that these protofibrils were derived directly from oligomers rather than from a small monomer pool in equilibrium with the oligomers following removal of SDS. In a previous study, incubation of Aβ(1−42) at high concentrations (100 μM) initially gave only oligomers but after a week gave a mixture of oligomers and short fibrils by AFM (*25*). Therefore, while we cannot rule out a very slow rate of conversion of these larger oligomers to protofibrils, our data indicate that the two pathways in Figure 8 are alternatives that do not intersect.

ACKNOWLEDGMENT

The authors thank Bernadette Cusack for her help with mass spectrometry.

REFERENCES

1. Cohen, A. S., and Calkins, E. (1959) Electron microscopic observation on a fibrous component in amyloid of diverse origins, *Nature 183*, 1202−1203.
2. Glenner, G. G., and Wong, C. W. (1984) Alzheimer's disease: Initial report of the purification and characterization of a novel

cerebrovascular amyloid protein, *Biochem. Biophys. Res. Commun. 120*, 885−890.
3. Miller, D. L., Papayannopoulos, I. A., Styles, J., Bobin, S. A., Lin, Y. Y., Biemann, K., and Iqbal, K. (1993) Peptide compositions of the cerebrovascular and senile plaque core amyloid deposits of Alzheimer's disease, *Arch. Biochem. Biophys. 301*, 41−52.
4. Selkoe, D. J. (2001) Alzheimer's disease: genes, proteins, and therapy, *Physiol. Rev. 81*, 741−766.
5. Hardy, J. A., and Higgins, G. A. (1992) Alzheimer's disease: the amyloid cascade hypothesis, *Science 256*, 184−185.
6. Selkoe, D. J., and Podlisny, M. B. (2002) Deciphering the genetic basis of Alzheimer's disease, *Annu. Rev. Genomics Hum. Genet. 3*, 67−99.
7. Nilsberth, C., Westlind-Danielsson, A., Eckman, C. B., Condron, M. M., Axelman, K., Forsell, C., Stenh, C., Luthman, J., Teplow, D. B., Younkin, S. G., Naslund, J., and Lannfelt, L. (2001) The 'Arctic' APP mutation (E693G) causes Alzheimer's disease by enhanced Aβ protofibril formation, *Nat. Neurosci. 4*, 887−893.
8. Hardy, J., and Selkoe, D. J. (2002) The amyloid hypothesis of Alzheimer's disease: Progress and problems on the road to therapeutics, *Science 297*, 353−356.
9. Hartley, D. M., Walsh, D. M., Ye, C. P., Diehl, T., Vasquez, S., Vassilev, P. M., Teplow, D. B., and Selkoe, D. J. (1999) Protofibrillar intermediates of amyloid β-protein induce acute electrophysiological changes and progressive neurotoxicity in cortical neurons, *J. Neurosci. 19*, 8876−8884.
10. Klein, W. L., Krafft, G. A., and Finch, C. E. (2001) Targeting small Aβ oligomers: The solution to an Alzheimer's disease conundrum? *Trends Neurosci. 24*, 219−224.
11. Westerman, M. A., Cooper-Blacketer, D., Mariash, A., Kotilinek, L., Kawarabayashi, T., Younkin, L. H., Carlson, G. A., Younkin, S. G., and Ashe, K. H. (2002) The relationship between Aβ and memory in the Tg2576 mouse model of Alzheimer's disease, *J. Neurosci. 22*, 1858−1867.
12. Kawarabayashi, T., Shoji, M., Younkin, L. H., Lin, W. L., Dickson, D. W., Murakami, T., Matsubara, E., Abe, K., Ashe, K. H., and Younkin, S. G. (2004) Dimeric amyloid β protein rapidly accumulates in lipid rafts followed by apolipoprotein E and phosphorylated tau accumulation in the Tg2576 mouse model of Alzheimer's disease, *J. Neurosci. 24*, 3801−3809.
13. Townsend, M., Shankar, G. M., Mehta, T., Walsh, D. M., and Selkoe, D. J. (2006) Effects of secreted oligomers of amyloid β-protein on hippocampal synaptic plasticity: a potent role for trimers, *J. Physiol. 572*, 477−492.
14. Lesne, S., Koh, M. T., Kotilinek, L., Kayed, R., Glabe, C. G., Yang, A., Gallagher, M., and Ashe, K. H. (2006) A specific amyloid-β protein assembly in the brain impairs memory, *Nature 440*, 352−357.
15. McLean, C. A., Cherny, R. A., Fraser, F. W., Fuller, S. J., Smith, M. J., Beyreuther, K., Bush, A. I., and Masters, C. L. (1999) Soluble pool of Aβ amyloid as a determinant of severity of neurodegeneration in Alzheimer's disease, *Ann. Neurol. 46*, 860−866.
16. Podlisny, M. B., Ostaszewski, B. L., Squazzo, S. L., Koo, E. H., Rydell, R. E., Teplow, D. B., and Selkoe, D. J. (1995) Aggregation of secreted amyloid β-protein into sodium dodecyl sulfate-stable oligomers in cell culture, *J. Biol. Chem. 270*, 9564−9570.
17. Walsh, D. M., Klyubin, I., Fadeeva, J. V., Cullen, W. K., Anwyl, R., Wolfe, M. S., Rowan, M. J., and Selkoe, D. J. (2002) Naturally secreted oligomers of amyloid β protein potently inhibit hippocampal long-term potentiation *in vivo*, *Nature 416*, 535−539.
18. Hsiao, K., Chapman, P., Nilsen, S., Eckman, C., Harigaya, Y., Younkin, S., Yang, F., and Cole, G. (1996) Correlative memory deficits, Aβ elevation, and amyloid plaques in transgenic mice, *Science 274*, 99−102.
19. Walsh, D. M., Townsend, M., Podlisny, M. B., Shankar, G. M., Fadeeva, J. V., El Agnaf, O., Hartley, D. M., and Selkoe, D. J. (2005) Certain inhibitors of synthetic amyloid β-peptide (Aβ) fibrillogenesis block oligomerization of natural Aβ and thereby rescue long-term potentiation, *J. Neurosci. 25*, 2455−2462.
20. Cleary, J. P., Walsh, D. M., Hofmeister, J. J., Shankar, G. M., Kuskowski, M. A., Selkoe, D. J., and Ashe, K. H. (2005) Natural oligomers of the amyloid-β protein specifically disrupt cognitive function, *Nat. Neurosci. 8*, 79−84.
21. Burdick, D., Soreghan, B., Kwon, M., Kosmoski, J., Knauer, M., Henschen, A., Yates, J., Cotman, C., and Glabe, C. (1992) Assembly and aggregation properties of synthetic Alzheimer's A4/beta amyloid peptide analogs, *J. Biol. Chem. 267*, 546−54.
22. Walsh, D. M., Lomakin, A., Benedek, G. B., Condron, M. M., and Teplow, D. B. (1997) Amyloid β-protein fibrillogenesis: Detection of a protofibrillar intermediate, *J. Biol. Chem. 272*, 22364−22372.
23. Lambert, M. P., Barlow, A. K., Chromy, B. A., Edwards, C., Freed, R., Liosatos, M., Morgan, T. E., Rozovsky, I., Trommer, B., Viola, K. L., Wals, P., Zhang, C., Finch, C. E., Krafft, G. A., and Klein, W. L. (1998) Diffusible, nonfibrillar ligands derived from Aβ_{1-42} are potent central nervous system neurotoxins, *Proc Natl Acad Sci U.S.A. 95*, 6448−6453.
24. Chromy, B. A., Nowak, R. J., Lambert, M. P., Viola, K. L., Chang, L., Velasco, P. T., Jones, B. W., Fernandez, S. J., Lacor, P. N., Horowitz, P., Finch, C. E., Krafft, G. A., and Klein, W. L. (2003) Self-assembly of Aβ(1−42) into globular neurotoxins, *Biochemistry 42*, 12749−12760.
25. Stine, W. B. J., Dahlgren, K. N., Krafft, G. A., and LaDu, M. J. (2003) *In vitro* characterization of conditions for amyloid-β peptide oligomerization and fibrillogenesis, *J. Biol. Chem. 278*, 11612−11622.
26. Barghorn, S., Nimmrich, V., Striebinger, A., Krantz, C., Keller, P., Janson, B., Bahr, M., Schmidt, M., Bitner, R. S., Harlan, J., Barlow, E., Ebert, U., and Hillen, H. (2005) Globular amyloid β-peptide(1−42) oligomer - a homogenous and stable neuropathological protein in Alzheimer's disease, *J. Neurochem. 95*, 834−847.
27. Yamamoto, N., Hasegawa, K., Matsuzaki, K., Naiki, H., and Yanagisawa, K. (2004) Environment- and mutation-dependent aggregation behavior of Alzheimer amyloid β-protein, *J. Neurochem. 90*, 62−69.
28. Rangachari, V., Reed, D. K., Moore, B. D., and Rosenberry, T. L. (2006) Secondary structure and interfacial aggregation of amyloid-β(1−40) on sodium dodecylsulfate micelles, *Biochemistry 45*, 8639−8648.
29. Abedini, A., and Raleigh, D. P. (2005) Incorporation of pseudoproline derivatives allows the facile synthesis of human IAPP, a highly amyloidogenic and aggregation-prone polypeptide, *Org. Lett. 7*, 693−696.
30. Fezoui, Y., Hartley, D. M., Harper, J. D., Khurana, R., Walsh, D. M., Condron, M. M., Selkoe, D. J., Lansbury, P. T., Jr., Fink, A. L., and Teplow, D. B. (2000) An improved method of preparing the amyloid β-protein for fibrillogenesis and neurotoxicity experiments, *Amyloid 7*, 166−178.
31. Nichols, M. R., Moss, M. A., Reed, D. K., Lin, W.-L., Mukhopadhyay, R., Hoh, J. H., and Rosenberry, T. L. (2002) Growth of β-amyloid(1−40) protofibrils by monomer elongation and lateral association. Characterization of distinct products by light scattering and atomic force microscopy, *Biochemistry 41*, 6115−6127.
32. Nielsen, L., Khurana, R., Coats, A., Frokjaer, S., Brange, J., Vyas, S., Uversky, V. N., and Fink, A. L., (2001) *Biochemistry 40*, 8397−8409.
33. Kukar, T., Murphy, M. P., and Eriksen, J. L., S. S., Weggen, S., Smith, T. E., Ladd, T., Khan, M. A., Kache, R., Beard, J., Dodson, M., Merit, S., Ozols, V. V., Anastasiadis, P. Z., Das, P., Fauq, A., Koo, E. H., Golde, T. E. (2005) Diverse compounds mimic Alzheimer disease-causing mutations by augmenting Aβ42 production, *Nat. Med. 11*, 545−550.
34. Suzuki, N., Cheung, T. T., Cai, X. D., Odaka, A., Otvos, L., Jr., Eckman, C., Golde, T. E., and Younkin, S. G. (1994) An increased percentage of long amyloid β protein secreted by familial amyloid β protein precursor (βAPP717) mutants, *Science 264*, 1336−1340.
35. LeVine, H. (1993) Thioflavine T interaction with synthetic Alzheimer's disease β-amyloid peptides: Detection of amyloid aggregation in solution, *Protein Sci. 2*, 404−410.
36. Nichols, M. R., Moss, M. A., Reed, D. K., Hoh, J. H., and Rosenberry, T. L. (2005) Amyloid-beta aggregates formed at polar-nonpolar interfaces differ from amyloid-beta protofibrils produced in aqueous buffers, *Microsc. Res. Tech. 67*, 164−174.
37. Harper, J. D., Wong, S. S., Lieber, C. M., and Lansbury, P. T., Jr. (1999) Assembly of Aβ amyloid peptides: An *in vitro* model for a possible early event in Alzheimer's disease, *Biochemistry 38*, 8972−8980.
38. Tseng, B. P., Esler, W. P., Clish, C. B., Stimson, E. R., Ghilardi, J. R., Vinters, H. V., Mantyh, P. W., Lee, J. P., and Maggio, J. E. (1999) Deposition of monomeric, not oligomeric, Aβ mediates growth of Alzheimer's disease amyloid plaques in human brain preparations, *Biochemistry 38*, 10424−10431.
39. Nichols, M. R., Moss, M. A., Reed, D. K., Cratic-McDaniel, S., Hoh, J. H., and Rosenberry, T. L. (2005) Amyloid-β protofibrils

differ from amyloid-β aggregates induced in dilute hexafluoroisopropanol in stability and morphology, *J. Biol. Chem. 280*, 2471−2480.
40. Hepler, R. W., Grimm, K. M., Nahas, D. D., Breese, R., Dodson, E. C., Acton, P., Keller, P. M., Yeager, M., Wang, H., Shughrue, P., Kinney, G., and Joyce, J. G. (2006) Solution state characterization of amyloid β-derived diffusible ligands, *Biochemistry 45*, 15157−15167.
41. Hilbich, C., Kisters-Woike, B., Reed, J., Masters, C. L., and Beyreuther, K. (1991) Aggregation and secondary structure of synthetic amyloid beta A4 peptides of Alzheimer's disease, *J. Mol. Biol. 218*, 149−63.
42. Walsh, D. M., Hartley, D. M., Kusumoto, Y., Fezoui, Y., Condron, M. M., Lomakin, A., Benedek, G. B., Selkoe, D. J., and Teplow, D. B. (1999) Amyloid β-protein fibrillogenesis: Structure and biological activity of protofibrillar intermediates, *J. Biol. Chem. 274*, 25945−25952.
43. Jarrett, J. T., Berger, E. P., and Lansbury, P. T., Jr. (1993) The carboxy terminus of the beta amyloid protein is critical for the seeding of amyloid formation: implications for the pathogenesis of Alzheimer's disease, *Biochemistry 32*, 4693−4697.
44. Reynolds, J. A., and Tanford, C. (1970) The gross conformation of protein-sodium dodecyl sulfate complexes, *J. Biol. Chem. 245*, 5161−5165.
45. Mattice, W. L., Riser, J. M., and Clark, D. S. (1976) Conformational properties of the complexes formed by proteins and sodium dodecyl sulfate, *Biochemistry 15*, 4264−4272.
46. Bisaglia, M., Trolio, A., Bellanda, M., Bergantino, E., Bubacco, L., and Mammi, S. (2006) Structure and topology of the non-amyloid-β component fragment of human α-synuclein bound to micelles: Implications for the aggregation process, *Protein Sci. 15*, 1408−1416.
47. Pertinhez, T. A., Bouchard, M., Smith, R. A., Dobson, C. M., and Smith, L. J. (2002) Stimulation and inhibition of fibril formation by a peptide in the presence of different concentrations of SDS, *FEBS Lett. 529*, 193−197.
48. Terzi, E., Holzemann, G., and Seelig, J. (1997) Interaction of Alzheimer β-amyloid peptide(1−40) with lipid membranes, *Biochemistry 36*, 14845−14852.
49. Schmechel, A., Zentgraf, H., Scheuermann, S., Fritz, G., Pipkorn, R., Reed, J., Beyreuther, K., Bayer, T. A., and Multhaup, G. (2003) Alzheimer β-amyloid homodimers facilitate Aβ fibrillization and the generation of conformational antibodies, *J. Biol. Chem. 278*, 35317−35324.
50. Knight, J. D., Hebda, J. A., and Miranker, A. D. (2006) Conserved and cooperative assembly of membrane-bound α-helical states of islet amyloid polypeptide, *Biochemistry 45*, 9496−9508.
51. Simons, K., and Vaz, W. L. (2004) Model systems, lipid rafts, and cell membranes, *Annu. Rev. Biophys. Biomol. Struct. 33*, 269−295.
52. Riddell, D. R., Christie, G., Hussain, I., and Dingwall, C. (2001) Compartmentalization of β-secretase (Asp2) into low-buoyant density, noncaveolar lipid rafts, *Curr. Biol. 11*, 1288−1293.
53. Wahrle, S., Das, P., Nyborg, A. C., McLendon, C., Shoji, M., Kawarabayashi, T., Younkin, L. H., Younkin, S. G., and Golde, T. E. (2002) Cholesterol-dependent gamma-secretase activity in buoyant cholesterol-rich membrane microdomains, *Neurobiol. Dis. 9*, 11−23.
54. Lee, S. J., Liyanage, U., Bickel, P. E., Xia, W., Lansbury, P. T., Jr, and Kosik, K. S. (1998) A detergent-insoluble membrane compartment contains A beta *in vivo*, *Nat. Med. 4*, 730−734.
55. Choo-Smith, L. P., Garzon-Rodriguez, W., Glabe, C. G., and Surewicz, W. K. (1997) Acceleration of amyloid fibril formation by specific binding of Aβ-(1−40) peptide to ganglioside-containing membrane vesicles, *J. Biol. Chem. 272*, 22987−22990.
56. Choo-Smith, L. P., and Surewicz, W. K. (1997) The interaction between Alzheimer amyloid β(1−40) peptide and ganglioside GM1-containing membranes, *FEBS Lett. 402*, 95−98.
57. Kakio, A., Nishimoto, S., Yanagisawa, K., Kozutsumi, Y., and Matsuzaki, K. (2002) Interactions of amyloid β-protein with various gangliosides in raft-like membranes: importance of GM1 ganglioside-bound form as an endogenous seed for Alzheimer amyloid, *Biochemistry 41*, 7385−7390.
58. Yamamoto, N., Hirabayashi, Y., Amari, M., Yamaguchi, H., Romanov, G., Van Nostrand, W. E., and Yanagisawa, K. (2005) Assembly of hereditary amyloid β-protein variants in the presence of favorable gangliosides, *FEBS Lett. 579*, 2185−2190.
59. Nichols, M. R., Moss, M. A., Reed, D. K., Hoh, J. H., and Rosenberry, T. L. (2005) Rapid assembly of amyloid-β peptide at a liquid/liquid interface produces unstable β-sheet fibers, *Biochemistry 44*, 165−173.
60. Bagriantsev, S. N., Kushnirov, V. V., and Liebman, S. W. (2006) Analysis of amyloid aggregates using agarose gel electrophoresis, *Methods Enzymol. 412*, 33−48.
61. Buck, M. (1998) Trifluoroethanol and colleagues: cosolvents come of age. Recent studies with peptides and proteins, *Q. Rev. Biophys. 31*, 297−355.
62. Atwood, C. S., Scarpa, R. C., Huang, X., Moir, R. D., Jones, W. D., Fairlie, D. P., Tanzi, R. E., and Bush, A. I. (2000) Characterization of copper interactions with Alzheimer amyloid β peptides: Identification of an attomolar-affinity copper binding site on amyloid β1−42, *J. Neurochem. 75*, 1219−1233.
63. Atwood, C. S., Perry, G., Zeng, H., Kato, Y., Jones, W. D., Ling, K. Q., Huang, X., Moir, R. D., Wang, D., Sayre, L. M., Smith, M. A., Chen, S. G., and Bush, A. I. (2004) Copper mediates dityrosine cross-linking of Alzheimer's amyloid-β, *Biochemistry 43*, 560−568.
64. Dudek, S. M., and Johnson, G. V. (1994) Transglutaminase facilitates the formation of polymers of the β-amyloid peptide, *Brain Res. 651*, 129−133.
65. Benzinger, T. L. S., Gregory, D. M., Burkoth, T. S., Miller-Auer, H., Lynn, D. G., Botto, R. E., and Meredith, S. C. (1998) Propagating structure of Alzheimer's β-amyloid$_{(10-35)}$ is parallel β-sheet with residues in exact register, *Proc. Natl. Acad. Sci. U.S.A. 95*, 13407−13412.
66. Boutaud, O., Montine, T. J., Chang, L., Klein, W. L., and Oates, J. A. (2006) PGH2-derived levuglandin adducts increase the neurotoxicity of amyloid β1−42, *J. Neurochem. 96*, 917−923.
67. Boutaud, O., Ou, J. J., Chaurand, P., Caprioli, R. M., Montine, T. J., and Oates, J. A. (2002) Prostaglandin H2 (PGH2) accelerates formation of amyloid β1−42 oligomers, *J. Neurochem. 82*, 1003−1006.
68. Bitan, G., Fradinger, E. A., Spring, S. M., and Teplow, D. B. (2005) Neurotoxic protein oligomers−what you see is not always what you get, *Amyloid 12*, 88−95.
69. Bitan, G., Kirkitadze, M. D., Lomakin, A., Vollers, S. S., Benedek, G. B., and Teplow, D. B. (2003) Amyloid β-protein (Aβ) assembly: Aβ40 and Aβ42 oligomerize through distinct pathways, *Proc. Natl. Acad. Sci. U.S.A. 100*, 330−335.
70. Williams, A. D., Sega, M., Chen, M., Kheterpal, I., Geva, M., Berthelier, V., Kaleta, D. T., Cook, K. D., and Wetzel, R. (2005) Structural properties of Aβ protofibrils stabilized by a small molecule, *Proc. Nat. Acad. Sci. U.S.A. 102*, 7115−7120.
71. Harper, J. D., Wong, S. S., Lieber, C. M., and Lansbury, P. T., Jr. (1997) Observation of metastable Aβ amyloid protofibrils by atomic force microscopy, *Chem. Biol. 4*, 119−125.
72. Goldsbury, C. S., Wirtz, S., Muller, S. A., Sunderji, S., Wicki, P., Aebi, U., and Frey, P. (2000) Studies on the *in vitro* assembly of Aβ 1−40: Implications for the search for Aβ fibril formation inhibitors, *J. Struct. Biol. 130*, 217−231.
73. Huang, T. H., Yang, D. S., Plaskos, N. P., Go, S., Yip, C. M., Fraser, P. E., and Chakrabartty, A. (2000) Structural studies of soluble oligomers of the Alzheimer beta-amyloid peptide, *J. Mol. Biol. 297*, 73−87.
74. Dahlgren, K. N., Manelli, A. M., Stine, W. B., Jr., Baker, L. K., Krafft, G. A., and LaDu, M. J. (2002) Oligomeric and fibrillar species of amyloid-β peptides differentially affect neuronal viability, *J. Biol. Chem. 277*, 32046−32053.
75. Necula, M., Kayed, R., Milton, S., and Glabe, C. G. (2007) Small-molecule inhibitors of aggregation indicate that amyloid beta oligomerization and fibrillization pathways are independent and distinct, *J. Biol. Chem. 282*, 10311−10324.

BI701213S